

# SN 2011ht: Confirming a Class of Interacting Supernovae with Plateau Light Curves (Type IIn-P)

Jon C. Mauerhan<sup>1\*</sup>, Nathan Smith<sup>1</sup>, Jeffrey M. Silverman<sup>2</sup>, Alexei V. Filippenko<sup>2</sup>, Adam N. Morgan<sup>2</sup>, S. Bradley Cenko<sup>2</sup>, Mohan Ganeshalingam<sup>2</sup>, Kelsey I. Clubb<sup>2</sup>, Thomas Matheson<sup>3</sup>

<sup>1</sup>*University of Arizona, Steward Observatory, Tucson, Arizona 85721, USA*

<sup>2</sup>*Department of Astronomy, University of California, Berkeley, CA 94720-3411, USA*

<sup>3</sup>*National Optical Astronomy Observatory, Tucson, AZ 85719, USA*

8 November 2018

## ABSTRACT

We present photometry and spectroscopy of the Type IIn supernova (SN) 2011ht, identified previously as a SN impostor — the eruption of a luminous blue variable (LBV). The light curve exhibits an abrupt transition from a well-defined  $\sim 120$  day plateau to a steep bolometric decline, plummeting 4–5 mag in the optical and 2–3 mag in the infrared in only  $\sim 10$  days. Leading up to peak brightness ( $M_V = -17.4$  mag), a hot emission-line spectrum exhibits strong signs of interaction with circumstellar material (CSM), in the form of relatively narrow P-Cygni features of H I and He I superimposed on broad Lorentzian wings. For the remainder of the plateau phase the spectrum exhibits strengthening P-Cygni profiles of Fe II, Ca II, and H $\alpha$ . By day 147, after the plateau has ended, the SN entered the nebular phase, heralded by the appearance of forbidden transitions of [O I], [O II], and [Ca II] over a weak continuum. At this stage, the light curve exhibits a low luminosity that is comparable to that of subluminous Type II-P supernovae (SNe II-P), and a relatively fast visual-wavelength decline that is significantly steeper than the  $^{56}\text{Co}$  decay rate. However, the total bolometric decline, including the infrared luminosity, is consistent with  $^{56}\text{Co}$  decay, and implies a low  $^{56}\text{Ni}$  mass of  $\sim 0.01 M_\odot$ . We therefore characterize SN 2011ht as a bona-fide core-collapse SN very similar to the peculiar SNe IIn 1994W and 2009kn. These three SNe define a subclass, which are Type IIn based on their spectrum, but that also exhibit well-defined plateaus and produce low  $^{56}\text{Ni}$  yields. We therefore suggest Type IIn-P as a name for this subclass. The absence of observational signatures of high-velocity material from these SNe could be the result of an opaque shell at the SN-CSM interface, which remains optically thick longer than the time scale for the inner ejecta to cool and become transparent. Possible progenitors of SNe IIn-P, consistent with the available data, include 8–10  $M_\odot$  stars, which undergo core collapse as a result of electron capture after a brief phase of enhanced mass loss; or more massive ( $M \gtrsim 25 M_\odot$ ) progenitors, which experience substantial fallback of the metal-rich radioactive ejecta. In either case, the energy radiated by these three SNe during their plateau ( $3 \times 10^{49}$  erg for SN 2011ht) must be dominated by CSM interaction.

**Key words:** supernovae: general — supernovae: individual (SN 2011ht)

## 1 INTRODUCTION

Type IIn supernovae (SNe IIn) are a subset of core-collapse events that exhibit relatively narrow emission lines in their spectra (Schlegel 1990; Filippenko 1997), indicating the

presence of dense circumstellar material (CSM) that envelops the SN explosion (Chugai 1990). This CSM, which masks the broad emission and absorption features typically seen in normal SNe, must have been ejected by the progenitor in the years to decades prior to explosion. The enhanced mode of pre-SN mass loss can occur over a large range of time scales, from eruptive events months to years before the

\* E-mail: mauerhan@as.arizona.edu

explosion, to long-duration superwinds that blow for millennia. As such, multi-epoch observations of SNe IIn allow us to probe the mass-loss parameters and physical states of the massive stars immediately preceding their core collapse, providing a unique glimpse into the final phase of massive-star evolution.

The progenitors of SNe IIn may span the entire range of massive-star classes, including luminous blue variables (LBVs; e.g., SN 2005gl, Gal-Yam & Leonard 2009; SN 2006tf, SN 2006gy, Smith et al. 2007, 2008), red supergiants (RSGs; e.g., SN 2005ip, Smith et al. 2009; SN 1998S, Bowen et al. 2000, Mauerhan & Smith 2012), Wolf-Rayet stars (e.g., SN 1985F; Filippenko & Sargent 1985, Begelman & Sarazin 1986), as well as transitional Ofpe/WN9 stars on their way to the Wolf-Rayet phase (e.g., Smith et al. 2012a). Even the least massive of stars that are capable of becoming core-collapse SNe ( $8\text{--}10 M_{\odot}$ ) might be able to generate a Type IIn explosion, a possibility considered in the case of the SN IIn 1994W (Sollerman et al. 1998). Thus, a diverse range of progenitors can potentially experience a highly enhanced degree of mass loss prior to exploding. Although the physical mechanisms responsible for triggering the pre-SN superwinds and LBV eruptions are not understood, their initiation appears to herald impending core collapse, although the time scales involved may vary significantly. The fact that SNe IIn comprise only  $\sim 9\%$  of all core-collapse events (Smith et al. 2011; Li et al. 2011) complicates this picture, as there is no clear explanation why only a small fraction of massive stars spanning a large progenitor mass range experience such a highly enhanced degree of mass loss immediately before exploding.

For SNe IIn, the magnitude of the emission from CSM interaction is sensitive mainly to the velocity of the SN shock and the pre-SN wind density. These parameters can span a broad range, depending on the nature of the progenitor and its mass-loss history. It is thus difficult to gauge the magnitude of radioactive-element synthesis, or lack thereof, until after CSM interaction has diminished substantially. Some SNe IIn, such as the exceptionally luminous SN 2006gy, maintain powerful CSM interaction for so long that any radioactive-decay emission would fade away before becoming discernible in the light curve. Other interacting SNe, such as SNe 1980K and 1998S, reveal the common radioactive light-curve slope at earlier times, but still maintain enough CSM emission at late times to complicate or prevent radioactive diagnosis (e.g., Milisavljevic et al. 2012; Mauerhan & Smith 2012). Finally, a rare subset of SNe IIn that exhibit plateaus in their light curves, similar in shape to those of SNe II-P, become exceptionally faint after the plateau, well below the typical luminosity of radioactive decay. The SN IIn 1994W is of this latter subset, exhibiting an exceptionally faint and steeply declining light curve during its nebular phase, after a well-defined plateau.

Multiple interpretations have been considered in attempting to discern the enigmatic properties of SN 1994W, including explosive pre-SN mass loss (Chugai et al. 2004) that was followed by an explosion having an exceptionally low  $^{56}\text{Ni}$  yield (Sollerman et al. 1998), as well as a non-SN interpretation of colliding stellar mass-loss shells (Dessart et al. 2009). Few SNe have exhibited the unusual combination of observational properties displayed by SN 1994W. The SN IIn 2009kn was recently considered by Kankare et al. (2012) to be a “twin” of SN 1994W, based on the spec-

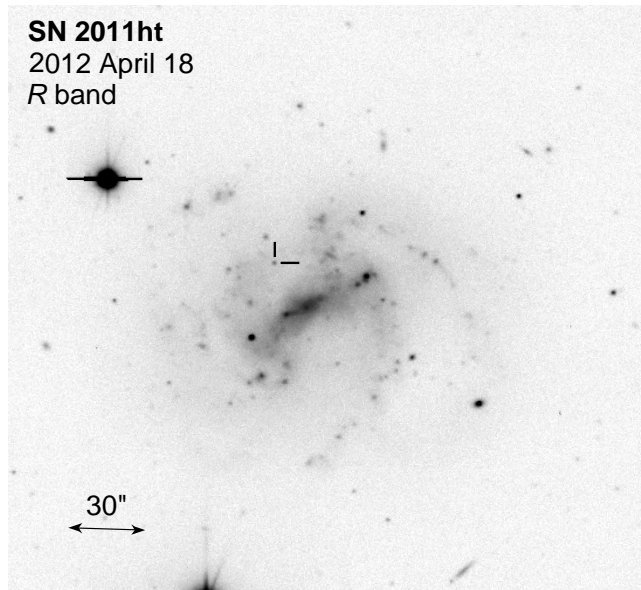


**Figure 1.** *R*-band image of UGC 4560 and SN 2011ht obtained with the 90Prime Imager on 2012 April 18 when the SN was at  $R = 20.77$  mag. North is up and east to the left.

tral morphology and a very similar well-defined plateau light curve. More recently, the discovery of SN 2011ht (Roming et al. 2011) has shown this SN to be an even closer twin of SN 1994W (Roming et al. 2012; Humphreys et al. 2012), exhibiting strikingly similar spectral evolution, a well-defined  $\sim 110\text{--}120$  day plateau, and an exceptionally faint and steeply declining optical decay tail.

Soon after discovery, SN 2011ht was identified as an unusual object. Initially, it was classified by Roming et al. (2011, ATEL 3690) as a possible SN “impostor” — the eruption of an LBV. This explosion was one of the first to be observed in the UV band during the rise to peak, revealing an extreme UV brightening of  $\sim 7$  mag, compared to  $\sim 2$  mag in the optical, which probably resulted from shock-breakout photons degraded by diffusion through dense CSM. X-ray emission detected with *Swift* was also reported by Roming et al. (2012), although subsequent high-resolution X-ray imaging with *Chandra* revealed that this was likely to be a false match with a background X-ray source (Pooley et al. 2012, ATEL 4062). The peak absolute visual magnitude of  $\sim -17$ , and early spectral evolution led to the conclusion that SN 2011ht was perhaps a true SN IIn, not an impostor (Prieto et al. 2011, CBET 2903). In further support of this interpretation, the total radiated energy of  $2.5 \times 10^{49}$  erg derived for SN 2011ht during the first 110 days is far more luminous than typical LBV eruptions, unless the latter have a much wider luminosity distribution than currently thought (see Smith et al. 2011). Still, Humphreys et al. (2012) have continued to favor the SN impostor hypothesis for SN 2011ht.

Here, we present photometric and spectroscopic observations of SN 2011ht. Based on the following analysis, and comparison with SN 1994W and SN 2009kn, we interpret SN 2011ht as a bona fide core-collapse event. As such, it helps solidify a new class of interacting SNe that exhibit

**Table 1.** Optical photometry of SN 2011ht. Epochs are given with respect to discovery date (2011 Sep. 29). The uncertainties represent the standard deviation of the zero-point magnitudes derived from measurements of 4–5 field stars.

JD−2,450,000 /Epoch (days)	<i>B</i> (mag)	<i>V</i> (mag)	<i>R</i> (mag)	<i>I</i> (mag)
5868.8/35	14.41(0.05)	14.46(0.14)	14.23(0.09)	14.18(0.08)
5873.8/40	14.32(0.05)	14.37(0.14)	14.15(0.09)	14.08(0.07)
5875.8/42	14.26(0.06)	14.38(0.15)	14.16(0.12)	14.13(0.11)
5879.5/46	14.28(0.05)	14.35(0.15)	14.15(0.13)	14.14(0.15)
5888.8/55	14.50(0.10)	14.26(0.17)	14.17(0.14)	14.16(0.14)
5893.5/60	14.37(0.06)	14.45(0.21)	14.24(0.18)	14.18(0.17)
5898.5/65	14.51(0.06)	14.59(0.21)	14.39(0.19)	14.21(0.21)
5901.5/68	14.52(0.06)	14.57(0.21)	14.34(0.17)	14.23(0.17)
5905.5/72	14.60(0.06)	14.64(0.21)	14.32(0.15)	14.24(0.17)
5912.5/79	14.71(0.05)	14.69(0.15)	14.46(0.14)	14.35(0.13)
5924.8/91	15.07(0.06)	14.95(0.21)	14.68(0.19)	14.52(0.20)
5933.5/100	15.46(0.04)	15.20(0.20)	14.85(0.20)	14.78(0.21)
5936.5/103	15.51(0.06)	15.23(0.21)	14.91(0.19)	14.69(0.19)
5943.5/110	15.80(0.06)	15.35(0.21)	15.03(0.19)	14.79(0.20)
5957.8/124	16.68(0.05)	15.88(0.15)	15.37(0.11)	15.03(0.12)
5961.5/128	17.38(0.06)	16.49(0.21)	15.94(0.19)	15.55(0.18)
5974.5/141	20.39(0.21)	19.96(0.20)	19.11(0.20)	18.48(0.21)
6036.5/203	...	21.39(0.25)	20.77(0.20)	20.37(0.15)
6054.6/221	...	...	21.43(0.15)	...

**Table 2.** PAIRITEL near-IR photometry of SN 2011ht. The uncertainties are statistical.

JD−2,450,000 /Epoch (days)	<i>J</i> (mag)	<i>H</i> (mag)	<i>K</i> (mag)
5861.5/28	14.23(0.03)	13.97(0.05)	13.72(0.08)
5864.5/31	14.05(0.02)	13.86(0.03)	13.61(0.06)
5866.5/33	14.00(0.02)	13.88(0.03)	13.67(0.09)
5882.5/49	13.92(0.02)	13.78(0.03)	13.51(0.05)
5888.4/55	13.89(0.02)	13.68(0.03)	13.43(0.05)
5892.4/59	13.88(0.03)	13.70(0.05)	13.62(0.09)
5894.4/61	13.86(0.02)	13.70(0.03)	13.48(0.07)
5900.5/67	13.94(0.02)	13.75(0.03)	13.62(0.04)
5903.5/70	13.94(0.02)	13.77(0.02)	13.54(0.04)
5922.4/89	14.09(0.02)	13.94(0.03)	13.65(0.06)
5928.4/95	14.11(0.02)	13.92(0.02)	13.63(0.06)
5932.4/99	14.17(0.02)	13.94(0.03)	13.70(0.06)
5936.4/103	14.21(0.03)	13.94(0.05)	13.82(0.14)
5949.4/116	14.34(0.02)	14.07(0.03)	13.83(0.06)
5953.4/120	14.33(0.02)	14.10(0.05)	13.97(0.09)
5959.4/126	14.66(0.02)	14.37(0.03)	14.17(0.06)
5961.4/128	15.01(0.06)	14.76(0.11)	14.61(0.23)
5964.3/131	16.04(0.07)	15.45(0.09)	...
5966.3/133	16.79(0.07)	16.59(0.12)	...
5968.4/135	16.77(0.10)	...	...
5977.4/144	18.28(0.25)	17.03(0.20)	16.28(0.2)

well-defined plateaus, spectra dominated by CSM interaction, and faint decay tails.

## 2 OBSERVATIONS

We began photometric monitoring of SN 2011ht roughly 28 days after its discovery date of 2011 Sep. 29. We obtained optical *BVRI* photometry using the 1 m Nickel telescope at Lick Observatory, and infrared (IR) *JHK* photometry using the 1.3 m Peters Automated Infrared Imaging Telescope (PAIRITEL)<sup>1</sup> on Mt. Hopkins (Bloom et al. 2006). The photometric measurements were obtained over 17–19

**Table 3.** Spectroscopic observations of SN 2011ht

JD−2,450,000 /Epoch (days)	Facility	Coverage (Å)	<i>R</i> $\delta\lambda/\lambda$
5860/26	Lick/Kast	3436–9920	1400, 900
5867/33	Keck/LRIS	3362–5630	1400
5867/33	Keck/LRIS	5740–7390	2200
5892/58	Lick/Kast	3436–9920	1400, 900
5898/64	Keck/LRIS	3362–5630	1400
5898/64	Keck/LRIS	5740–7390	2200
5914/80	Lick/Kast	3436–9920	1400, 900
5921/88	Keck/LRIS	3362–5630	1400
5921/88	Keck/LRIS	5740–7390	2200
5922/89	Lick/Kast	3436–9920	1400, 900
5928/96	MMT/BlueCh	5550–7500	4500
5929/96	Lick/Kast	3436–9920	1400, 900
5944/111	Lick/Kast	3436–9920	1400, 900
5946/113	MMT/BlueCh	5550–7500	4500
5956/123	MMT/BlueCh	5550–7500	4500
5958/125	Lick/Kast	3436–9920	1400, 900
5961/127	KPNO/RCSpec	3600–8270	1100
5981/147	Lick/Kast	3436–9920	1400, 900
5981/147	Keck/LRIS	3362–5630	1400
5981/147	Keck/LRIS	5740–7390	2200
5988/155	MMT/BlueCh	5550–7500	4500
6034/201	MMT/BlueCh	3920–8998	500
6036/202	Lick/Kast	3436–9920	1400, 900
6046/213	Keck/LRIS	5740–7390	2200
6071/238	MMT/BlueCh	5550–7500	4500

separate epochs between days 28–150 after discovery. Late-time photometry on days 203 and 221 was also obtained using the 90Prime Imager on the Bok 90" telescope on Kitt Peak, and the MONT4K Imager on the Kuiper 61" telescope on Mt. Bigelow, respectively. The Lick and PAIRITEL photometry was extracted using standard aperture-photometry techniques and calibrated by photometry of 4–6 field stars in the same image as the SN, while the late-time 90Prime and MONT4K photometry was extracted via point-spread-function (PSF) fitting with the IDL Starfinder code, in which case the host galaxy was modeled as local background, allowing for a more precise determination of the faint SN flux. Tables 1 and 2 list the results.

Our spectroscopic monitoring campaign of SN 2011ht utilized the Kast spectrograph (Miller & Stone 1993) on the 3 m Shane reflector at Lick Observatory, the Low Resolution Imaging Spectrometer (LRIS; Oke et al. 1995) on the Keck I 10 m telescope, and the Bluechannel spectrograph on the Multiple Mirror Telescope (MMT), and the RC Spectrograph (RCSpec<sup>2</sup>) on the Mayall 4 m reflector at Kitt Peak National Observatory (KPNO). The spectroscopic observations are summarized in Table 3. The Lick/Kast spectra have moderate resolution ( $R \equiv \delta\lambda/\lambda \approx 900$  and 1400 for the red and blue sides of the Kast spectra, respectively) and covered a large wavelength range of 3436–9920 Å. The Keck/LRIS and MMT/Bluechannel spectra have higher spectral resolutions of  $R \sim 2200$  and 4500, respectively. The RCSpec spectra cover a wavelength range of 3200–8270 Å with a spectral resolution of  $\sim 1100$ . All spectra were generally obtained at low airmass or with an atmospheric dispersion corrector; otherwise, observations were performed with the slit at the parallactic angle in order to minimize chromatic differential slit losses (Filippenko 1982). Our data reduction, wavelength and flux calibration followed stan-

<sup>1</sup> See <http://www.pairitel.org/>.

<sup>2</sup> <http://www.noao.edu/kpno/manuals/rcspec/rcsp.html>

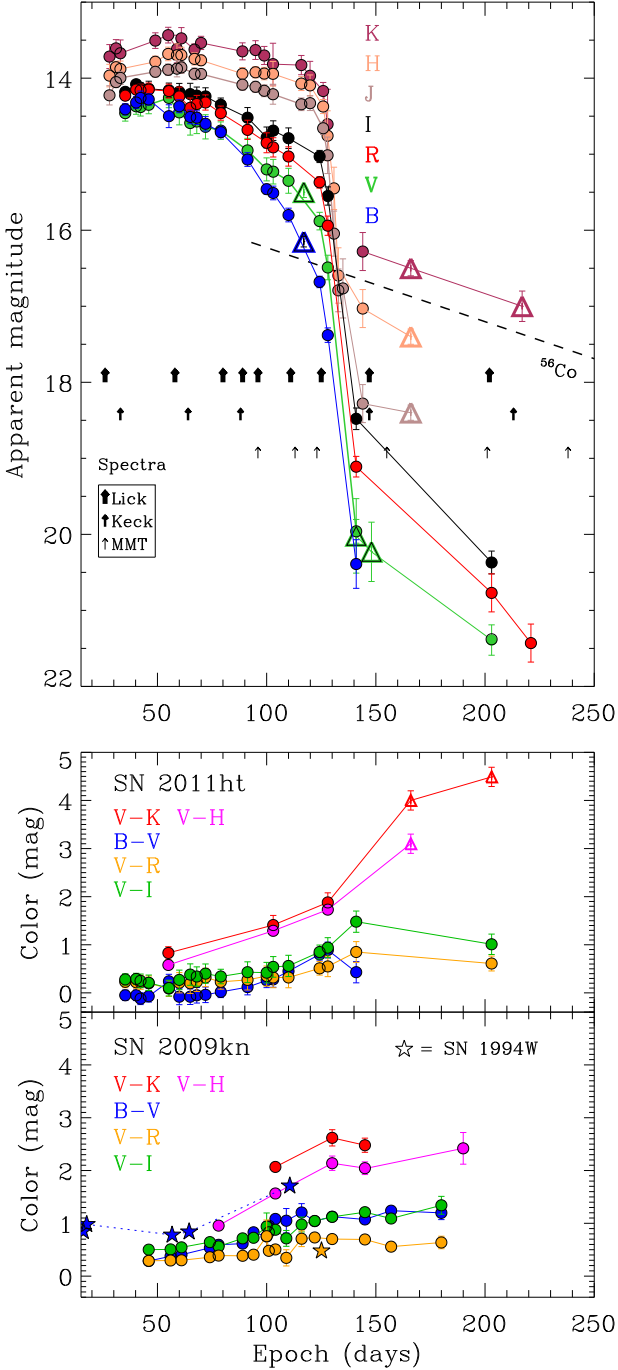


**Figure 2.** *BVRIJHK* light and color curves of SN 2011ht, with supplemental data from Humphreys et al. (2012; *triangles*). The color curves of SN 2009kn and SN 1994W (from Kankare et al. 2012) have been included for comparison. Epochs having accompanying spectra are marked with upward arrows. The dashed line exhibits the decline rate of  $^{56}\text{Co}$  decay, for an arbitrary  $^{56}\text{Ni}$  mass.

dard techniques as described by Silverman et al. (2012). Lick/Kast spectra of SN 2009kn, acquired and reduced utilizing the same instruments setting and reduction techniques described above, were also obtained on 2009 Nov 10 and Dec 9.

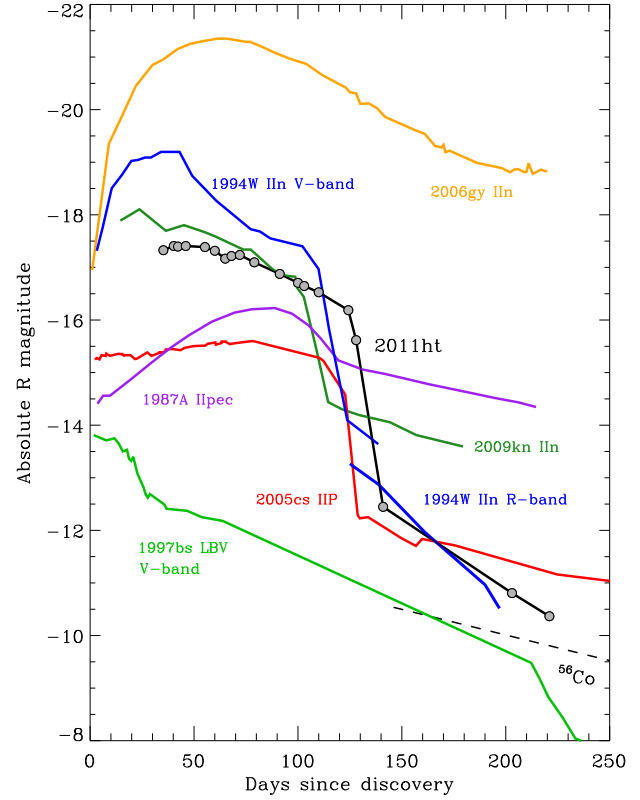


**Figure 3.** Absolute light curve of SN 2011ht, including comparison SNe 1994W (IIn; Sollerman et al. 1998), 2009kn (IIn; Kankare et al. 2012), 2005cs (II-P, Pastorello et al. 2009), 1987A (II-pec, Hamuy et al. 1990), and 2006gy (Smith et al. 2007), as well as LBV SN “impostor” 1997bs (Van Dyk et al. 2000). The height of the SN 2011ht plateau is typical of SNe IIn, but the late-time tail appears significantly subluminal and declines at a relatively rapid rate, like SN 1994W. The dashed line exhibits the decline rate of  $^{56}\text{Co}$  decay, for an arbitrary  $^{56}\text{Ni}$  mass.

### 3 RESULTS

#### 3.1 The Light Curve

The optical and IR light curves of SN 2011ht are presented in Figure 2. The first 20–30 days of monitoring cover the rise to maximum light followed by an extended 120-day plateau phase. The optical light curves peak near day 45 and the IR curves peak approximately two weeks later, near day 60. Between days 60 and 120, the optical curves begin a shallow decline that steepens with decreasing wavelength. In the *B* band, the curve gradually drops  $\sim 2$  mag before the end of the plateau on day  $\sim 120$ , while the *JHK* curves maintain relatively constant brightness for the entire duration of the plateau. By day 130, the light curve has begun a rapid descent of 4–5 mag in the optical and 2–3 mag in the infrared over a time scale of  $\sim 10$  days. By day  $\sim 140$ , a floor has been reached and the light curves subsequently exhibit a steady decline that continues through at least day 221.

The color curves at the bottom of Figure 2 illustrate the gradual intrinsic reddening of the SN during the plateau phase, as the flux at shorter wavelengths decreases the

fastest. Once the plateau phase has ended, however, the optical colors (including  $V - I$ ) flatten out, becoming slightly bluer. However, there is a substantial shift of flux toward the IR during the nebular phase, as evidenced by the continually increasing  $V - H$  and  $V - K$  curves. SN 2009kn and SN 1994W exhibit similar color trends in the optical and IR (Kankare et al. 2012), although the late-time IR coverage is not as complete as it is for SN 2011ht.

We computed the absolute magnitude of SN 2011ht, adopting an extinction value of  $A_V = 0.19$  mag and a distance of 19.2 Mpc to the host galaxy UCG 5460 (Romig et al. 2012), which yielded values of  $M_V = -17.35$  and  $M_R = -17.41$  mag at the respective peaks of days 55 and 46. We also derived the total integrated luminosity of the SN 2011ht plateau by calculating bolometric corrections using our measured optical colors in conjunction with the method described by Bersten et al. (2009), which is valid only for the plateau phase. Using the extinction-corrected  $B - V$  and  $V - I$  colors, two independent values of bolometric luminosity were computed for every epoch during the plateau and the results were averaged. The average difference between the two color-dependent luminosity values over all epochs was 0.36 dex. The resulting peak luminosity near day 55 is  $L_{\text{peak}} = (5 \pm 2) \times 10^{42} \text{ erg s}^{-1}$ , which is consistent with the peak luminosity reported by Romig et al. (2012). We then computed the total radiated energy of the plateau using trapezoidal integration, which yielded a total energy of  $E_{\text{rad,p}} \approx 3 \times 10^{49} \text{ erg}$ . Since this method did not account for the IR luminosity, it can be considered a lower limit. Nonetheless, the value is high, much higher than that of most SN impostors (Smith et al. 2011), although normal for core-collapse SNe.

The absolute light curve of SN 2011ht is presented in Figure 3, along with the those of various other core-collapse SNe and a SN impostor for comparison. The well-defined steep-edge plateau of SN 2011ht closely resembles that of the SNe IIn 2009kn and SN 1994W, although the early half of the plateau of SN 1994W was 1.5 mag brighter. The plateaus of each have similar durations of  $\sim 110$ –120 days and subsequently drop by a comparable magnitude. Plateaus with edges this sharp are not a typical characteristic of SNe IIn. However, the plateau durations of SNe 2011ht, 1994W, and 2009kn are very common to normal SNe II-P (Hamuy 2003). The subsequent decay tails of these SNe are relatively faint compared with those of most SNe IIn and II-P. The luminosities are comparable to a class of subluminous SNe II-P, such as SN 2005cs (Pastorello et al. 2004) and SN 2003Z (Utrobin et al. 2007). The optical decline rates of SN 2011ht and SN 1994W are also relatively steep, at 0.03–0.05 mag day $^{-1}$ . This behavior is uncharacteristic of normal SNe II-P, more similar to H-deficient SNe Ib/c, which typically exhibit faster decline rates of 0.01–0.02 mag day $^{-1}$  (Elmhamdi et al. 2011); still, SNe 2011ht and 1994W decline substantially more rapidly than even those objects.

Although the post-plateau optical decline of SN 2011ht is unusually steep, the available  $K$ -band measurements during this phase (from Humphreys et al. 2012), also shown in Figure 2, appear to be consistent with the  $^{56}\text{Co}$  decay rate. The much smaller drop in brightness for the IR after the plateau suggests that a substantial amount of optical flux has been reprocessed and shifted to longer wavelengths. So, to obtain a more precise estimate of the post-plateau

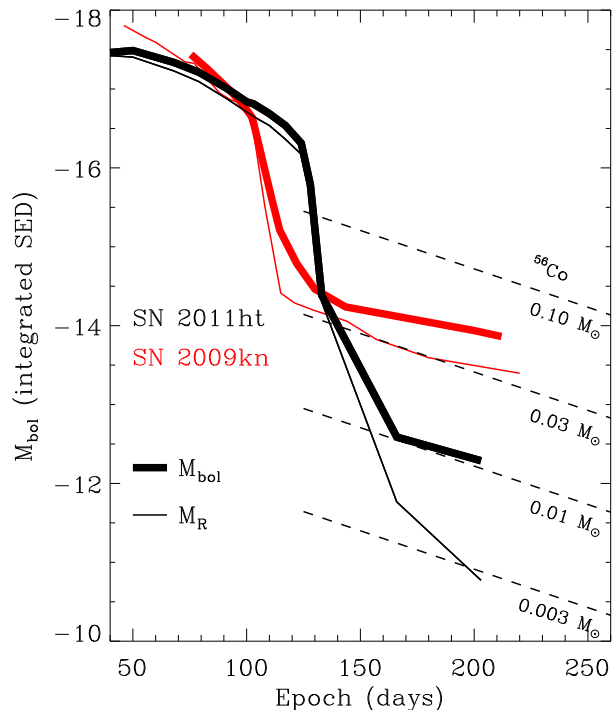


**Figure 4.** Absolute, bolometric (thick lines) and  $R$ -band (thin lines) light curves of SN 2011ht and SN 2009kn. The bolometric curves were derived by integrating the SEDs of both SNe between the optical  $B$  and IR  $K$  bands. In the case of SN 2011ht, the slope of the late bolometric tail matches the rate of  $^{56}\text{Co}$  decay (dashed lines), even though the individual  $R$ -band tail does not. The result suggests that the unusually steep late-time decline in the optical could be the result of flux shifting to longer wavelengths at late times. The  $^{56}\text{Co}$  decay curves are shown for  $^{56}\text{Ni}$  masses of 0.003, 0.01, 0.03, and  $0.1 M_{\odot}$ .

bolometric luminosity of SN 2011ht and SN 2009kn, we integrated their extinction-corrected spectral-energy distributions (SEDs) between the  $B$  and  $K$  bands (between  $V$  and  $K$  for SN 2011ht), adopting SN 2009kn measurements from Kankare et al. (2012). To match the available IR data of SN 2011ht from Humphreys et al. (2012) on day 166, we estimated the optical photometry of SN 2011ht by linearly interpolating between our measured points on days 141 and 203. For epoch 203, for which we have secure  $VRI$  detections, we interpolated the  $K$ -band photometry along the line connecting the measurements on days 166 and 217 from Humphreys et al. (2012).

The resulting bolometric light curves of SN 2011ht and SN 2009kn are presented in Figure 4, along with the absolute  $R$ -band curves for comparison. The actual luminosities could be slightly higher as a result of flux blueward of the  $V$  band and redward of the  $K$  band. Nonetheless, the results suggest that although the *optical* decay tail of SN 2011ht may exceed the decline rate of  $^{56}\text{Co}$  decay, the total bolometric luminosity, including the IR flux, declines at a rate fully consistent with  $^{56}\text{Co}$  decay. The absolute luminosities of the decay tails, however, are relatively faint compared with most SNe IIn and II-P, which implies a lower than average mass of  $^{56}\text{Ni}$ . The behavior of SN 2011ht, like SN 2009kn, is thus

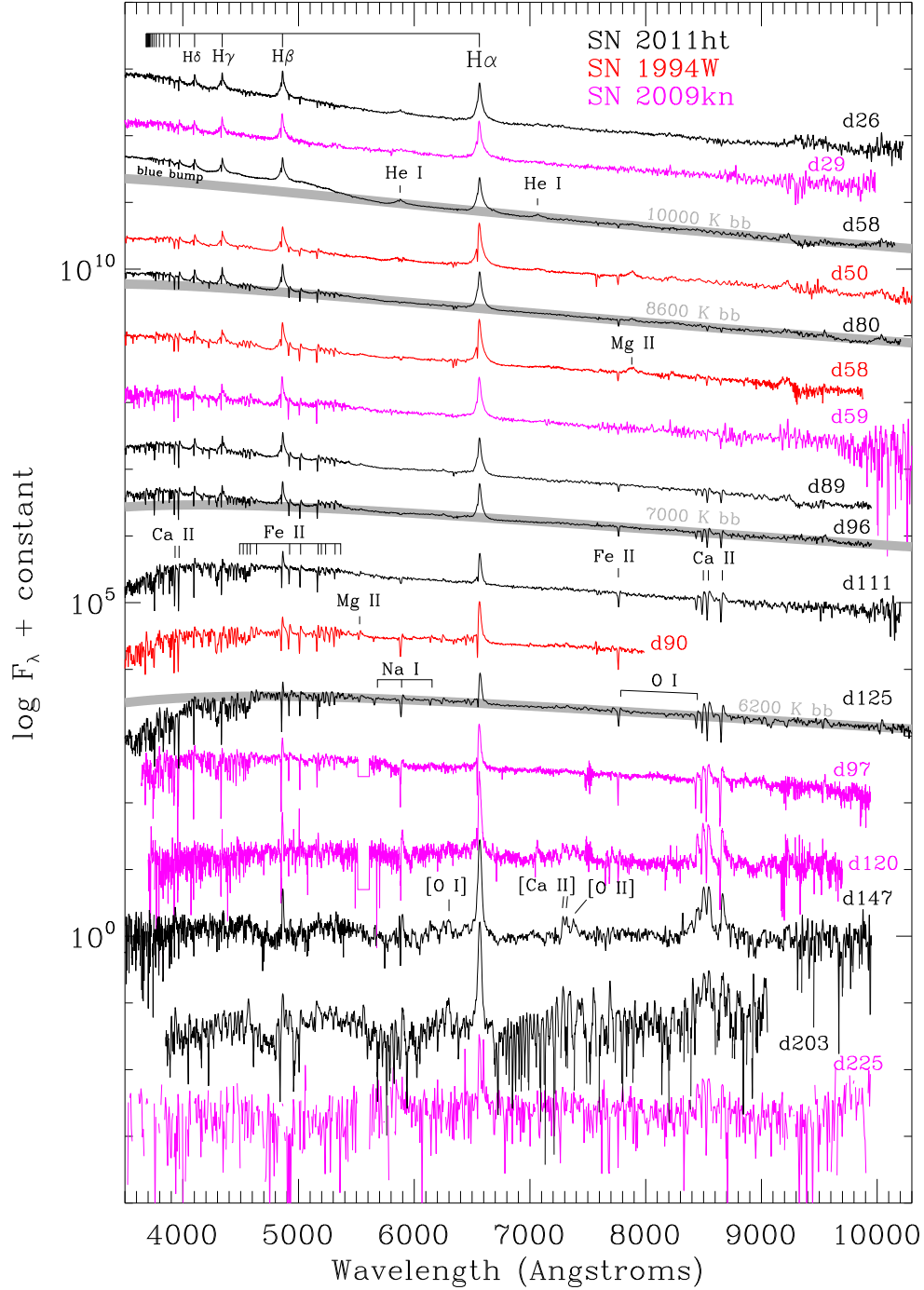


**Figure 5.** Dereddened spectra of SN 2011ht, with spectra of SN 1994W (red) and SN 2009kn (magenta) for comparison. The SN 1994W spectra were obtained from the Weizmann interactive SN data repository (Yaron & Gal-Yam 2012). Our own SN 2009kn spectra for days 29 and 59 are supplemented with spectra from days 97, 120, and 225 (Kankare et al. 2012), kindly provided by E. Kankare.

consistent with that of a bona fide core-collapse SN. The total bolometric luminosity of the plateau alone is, again,  $E_{\text{rad,p}} \approx 3 \times 10^{49}$  erg, consistent with the above method using only the optical photometry. Therefore, inclusion of the IR SED appears to be important only for estimating the bolometric flux during the post-plateau phase.

### 3.2 Spectral Evolution

Our Lick/Kast spectra of SN 2011ht and SN 2009kn are presented in Figure 5, in addition to three later epochs of SN 2009kn from Kankare et al. (2012), and archival spectra of SN 1994W from Chugai et al. (2004). Figure 6

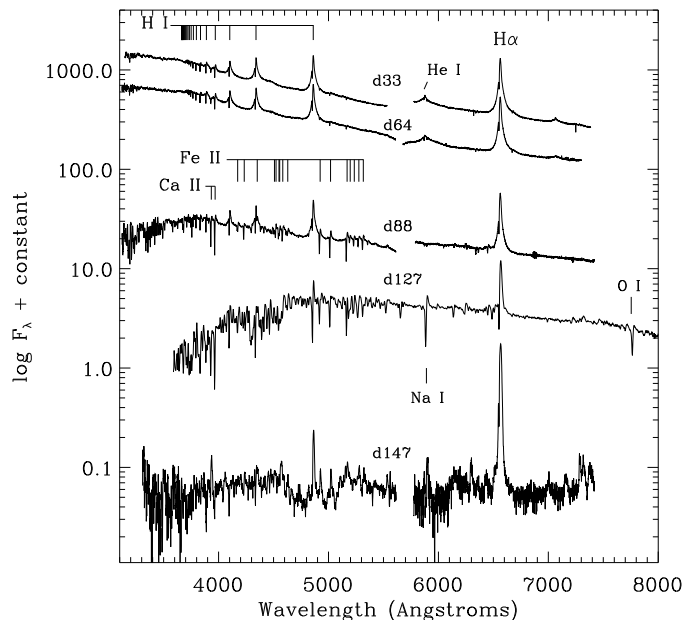


**Figure 6.** Optical spectra of SN 2011ht from Keck/LRIS, and a KPNO/RCSpec spectrum from day 127.

shows our higher-resolution spectra from Keck/LRIS and KPNO/RCSpec. Figure 7 displays the same Keck/LRIS spectra, in addition to our MMT spectra, all centered on the  $H\alpha$  emission line.

During the earliest epoch on day 26, SN 2011ht exhibits a characteristic SN IIn emission-line spectrum, dominated by the Balmer series of H I. The emission lines exhibit intermediate-width cores of full width at half-maximum intensity (FWHM)  $\sim 1500 \text{ km s}^{-1}$  on top of broad Lorentzian wings, which presumably form as a result of Thomson scattering of photons off of free electrons in the dense CSM and within the post-shock gas (Chugai et al. 2001; Dessart et al. 2009). The  $H\alpha$  emission peak is slightly asymmetric toward the red, consistent with the Roming et al. (2012) result. The underlying broad components have full-width near zero intensity (FWZI) values of  $8000\text{--}9000 \text{ km s}^{-1}$  on day 33, and weaken to  $\sim 7000 \text{ km s}^{-1}$  by day 64. The lines exhibit narrow P-Cygni absorption components with blueshifted velocities of  $\sim 500\text{--}600 \text{ km s}^{-1}$ , which remain at roughly constant velocity throughout the entire plateau phase. Weak emission from He I  $\lambda 5876$  is present at the earliest epochs and strongest on day 58. Weak absorption features of Fe II and Ca II H&K are present by day 80, in addition to weak Mg II  $\lambda 7888$  in pure emission. By day 58 (when the light curve is near maximum) the spectrum has increased in ionization temperature, with the strengthening of He I  $\lambda 5876$  and the appearance of He I  $\lambda 7065$ , in addition to the development of a strong blue excess that rises shortward of  $5500 \text{ \AA}$ . The excess begins near a cluster of Fe II lines, which become individually distinguishable as absorption-dominated P-Cygni features by day 80 and are accompanied by additional absorption features of this species in between  $H\beta$  and  $H\gamma$ . Redward of this bump the slope of the continuum appears to be consistent with a  $10,000 \text{ K}$  blackbody.

The Balmer lines and Fe II P-Cygni features appear in greater detail in our higher-resolution spectra (Fig. 6),

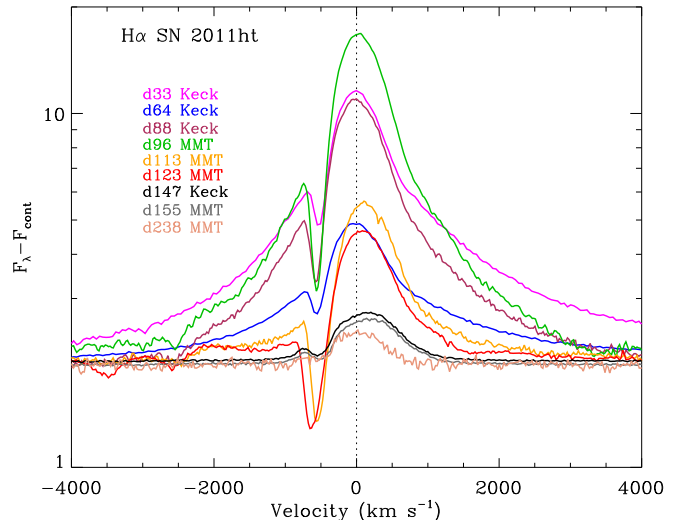


**Figure 7.** Evolution of the continuum-subtracted  $H\alpha$  profile of SN 2011ht between days 33 and 238 after discovery. At early times, the emission line exhibits an intermediate-width ( $\sim 1500 \text{ km s}^{-1}$ ) core P-Cygni profile with superimposed broad Lorentzian wings. At later times, the wings diminish, yet P-Cygni absorption remains present well into the nebular phase.

revealing that the Fe II lines also exhibit signs of Lorentzian broadening. Thus, the blue excess from day 58 appears to be the result of blended Fe II emission features, like SN 2005ip (Smith et al. 2009) and SN 2006jc (Chugai 2009).

On day 89, the spectrum has begun to exhibit the characteristics of a cool, dense gas, very similar to SN 1994W on day 58 and SN 2009kn on day 59. Continuously strengthening Fe II features are accompanied by P-Cygni lines of the Ca II triplet at  $7500\text{--}8000 \text{ \AA}$ , all of which continue to increase in strength through days 125–127, at which point Na I P-Cygni and absorption features also become evident. By this time, the continuum temperature has decreased to  $\sim 6200 \text{ K}$ , and the broad Lorentzian wings of  $H\alpha$  have become diminished beyond detectability, as evidenced by the higher-resolution spectra of  $H\alpha$  shown in Figure 7. In addition, metal-line blanketing suppresses the flux at the blue end of the spectrum, which must be at least partially responsible for the greater drop in the  $B$ -band light curve in Figure 2 (in addition to a decrease in blackbody temperature), before the plateau edge has been reached.

The spectrum on day 147, at which time the light curve exhibits a steady decline, indicates that the SN has entered the nebular phase. At this point, the continuum has weakened substantially, and the P-Cygni profiles are less prominent, although the higher-resolution  $H\alpha$  spectrum in Figure 7 shows that P-Cygni absorption is still present. The Balmer series has weakened significantly, with only  $H\alpha$ ,  $H\beta$ , and  $H\gamma$  clearly visible. Forbidden transitions of [O I], [O II], and [Ca II] have also appeared, the latter of which implies very low density for the gas. All emission lines remain narrow ( $< 1200 \text{ km s}^{-1}$ ) throughout our spectroscopic coverage of the nebular phase.

Using the distance and extinction values that we adopted to generate the absolute-magnitude curve in Figure 3, we calculated the luminosity of the  $H\alpha$  and  $H\beta$  emission lines, and compared it with those of SN 1994W (data

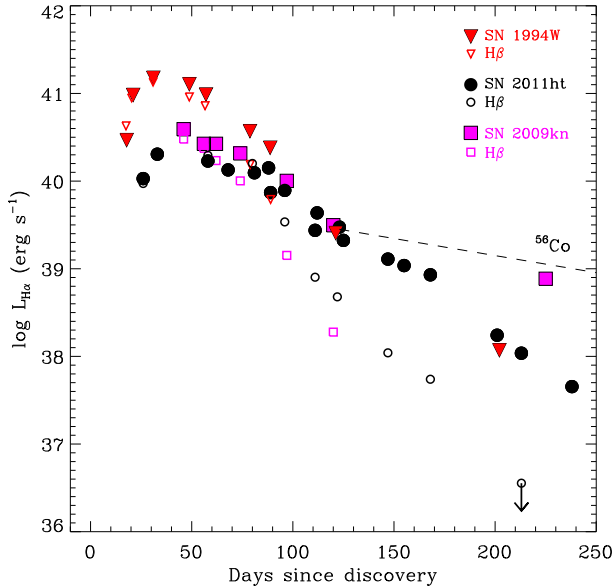


**Figure 8.** Light curves of  $H\alpha$  and  $H\beta$  luminosity for SNe 2011ht, 1994W, and 2009kn. SN 1994W is relatively luminous during its plateau, although each object converges to the same post-plateau  $H\alpha$  luminosity around day 120. The late-time declines of SNe 2011ht and 1994W are identical, at least out to day 203, and are steeper than SN 2009kn.

from Chugai et al. 2004) and SN 2009kn (Kankare et al. 2012). The results are presented in Figure 8. SN 1994W has a substantially higher  $H\alpha$  luminosity than SN 2011ht and SN 2009kn during the plateau phase, by almost an order of magnitude, which could be the result of interaction with higher-density CSM surrounding SN 1994W, a higher CSM filling factor (i.e., clumping), or geometric differences. After their plateau phases end around  $\sim 120$  days, the light curves of each SN converge to the same late-time  $H\alpha$  luminosity. The  $H\alpha$  decline rates of SN 2011ht and SN 1994W are identical throughout their nebular phases, and are steeper than SN 2009kn. The fact that the line emission does not exhibit the same sharp plateau edge as the broad-band light curves of these SNe suggests that the continuum and  $H\alpha$  emission source might not be coupled.

After the plateau,  $H\beta$  becomes noticeably fainter than  $H\alpha$  for each SN, corresponding to a rather instantaneous change in Balmer decrement. During the remainder of the nebular phase,  $H\beta$  exhibits approximately steady decline, somewhat steeper than for  $H\alpha$ .

## 4 DISCUSSION

SNe 2011ht, 1994W, and 2009kn share an unusual set of properties, particularly the combination of a luminous well-defined plateau light curve, a faint decay tail, and nearly identical spectral evolution that is distinct from the larger class of SNe IIn. The unique character of these three SNe suggests that a very specific physical scenario has played out in each of these events, involving circumstellar interaction and low  $^{56}\text{Ni}$  yield. The striking similarities shared by SNe 2011ht, 1994W, and 2009kn suggest that these are

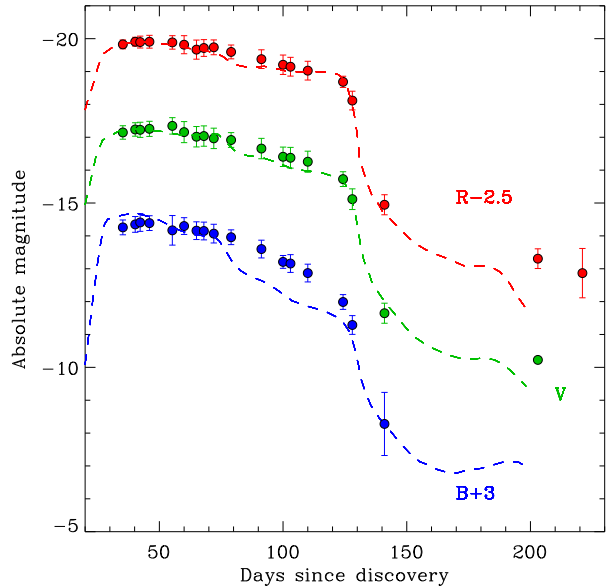


**Figure 9.**  $BV$  light curves of SN 2011ht plotted against a scaled CSM-interaction light-curve model for the SN IIn 1994W from Chugai et al. (2004).

the same type of explosion, whatever the underlying physics might be. Various possibilities are discussed below.

### 4.1 Circumstellar Interaction

The photometric and spectroscopic evolution of SN 2011ht during the plateau phase, specifically the high luminosity and the relatively narrow P-Cygni emission-line profiles superimposed on the broad Lorentzian wings, indicates strong interaction with CSM. SN 1994W exhibited a nearly identical spectral morphology and evolution, and modeling of this SN by Chugai et al. (2004) demonstrated that homologous expansion of dense CSM is required to fit the observational data. Additional modeling of this SN by Dessart et al. (2009) resulted in different conclusions about the origin of the spectral features, but also found that CSM interaction produced a good match to the spectrum.

The Chugai et al. (2004) model concluded that the CSM of SN 1994W consists of a  $0.4 M_{\odot}$  envelope having an accelerated velocity gradient of  $170\text{--}400 \text{ km s}^{-1}$  within a radius of  $3.3 \times 10^{15} \text{ cm}$ , which implies a very high mass-loss rate of  $0.3 M_{\odot} \text{ yr}^{-1}$  that probably occurred  $\sim 1.5 \text{ yr}$  before core collapse. Such a large mass-loss rate is beyond the physical parameters of a sustainable line-driven stellar wind, and implies an eruptive/explosive origin for the CSM (Smith & Owocki 2006). The observational characteristics of SNe 2011ht and 2009kn are so similar to those of SN 1994W that one could reasonably arrive at a similar physical interpretation for these SNe.

Figure 9 shows the best-fit model light curves for SN 1994W from Chugai et al. (2004) — specifically, their model “sn94w43”. To match the SN 2011ht data, we shifted the SN 1994W models down by a factor of 6–7 in luminosity ( $\sim 2 \text{ mag}$ ) and forward in time by 16 days (perhaps accounting for uncertainties in the explosion dates). For the  $R$  and

$V$  bands, the model plateau shape and the abrupt transition into the tail phase matches the SN 2011ht photometric data well, although the match to the  $B$ -band plateau data is not as satisfactory for the latter half of the plateau.

Although the SN 2011ht data match the overall shape of the SN 1994W model light curve, the factor of 6–7 discrepancy in peak  $H\alpha$  luminosity must be accounted for. Assuming strong interaction between a SN shock and surrounding CSM during the plateau phase, the luminosity of  $H\alpha$  can be expressed as

$$L(H\alpha) \propto \frac{L_s}{T_s} \propto \frac{V_s^3}{T_s} \left( \frac{\dot{M}}{v_w} \right), \quad (1)$$

where  $L_s$ ,  $T_s$ , and  $V_s$  are the shock ionizing luminosity, temperature, and velocity (respectively), and  $w = \dot{M}/v_w$  is the wind-density parameter. For SN 1994W, Chugai et al. (2004) estimated the shock velocity to be  $4000 \text{ km s}^{-1}$  and the shock temperature to be within a reasonable range of  $1\text{--}2 \times 10^4 \text{ K}$ . Their model, which requires a  $0.3 \text{ M}_\odot \text{ yr}^{-1}$  mass-loss rate and  $400 \text{ km s}^{-1}$  wind velocity, implies a very high wind-density parameter. Because of the high sensitivity of  $H\alpha$  emission to shock velocity, a factor of less than 2 difference in  $V_s$  alone could account for the factor of 6–7 lower luminosity of  $H\alpha$ , assuming the CSM wind-density parameters were similar for SN 2011ht and SN 1994W. This could be achievable by either an intrinsically faster shock, or a bigger velocity difference between the shock and the expanding CSM. Alternatively, if the shock velocities (and temperatures) are the same, which is supported by the very similar plateau durations, then the luminosity differences could instead indicate a lower-density CSM, or a lower geometric covering factor (solid angle) associated with the CSM of SN 2011ht. Assuming that differences in the CSM velocity between SN 2011ht and SN 1994W could be traced approximately by the relative blueshifts of their  $H\alpha$  P-Cygni absorption components, then the factor of 1.5 smaller blueshift for SN 2011ht would imply a factor of  $\sim 1.5$  increase in  $H\alpha$  luminosity. The fact that  $H\alpha$  is nearly an order of magnitude fainter for SN 2011ht during the plateau thus requires an order of magnitude lower mass-loss rate for the progenitor, or  $0.03 \text{ M}_\odot \text{ yr}^{-1}$ . This value is still extremely high, however, and thus would also imply an eruptive/explosive origin for the CSM associated with SN 2011ht.

The luminosity and decline rate of  $H\alpha$  during the nebular phase is practically identical for SN 2011ht and SN 1994W. In the latter case, Chugai et al. (2004) used the late-time  $H\alpha$  luminosity to constrain the outer pre-eruption wind parameters of the progenitor. The low luminosity of SN 1994W on day 203 ( $L \approx 10^{38} \text{ erg s}^{-1}$ ) implies that the outer wind should have a density  $\sim 10$  and  $\sim 2$  times lower than that of the well-studied SN 1979C and SN 1980K (respectively), which presumably had red-supergiant progenitors (Fesen & Becker 1990; Weiler et al. 1991). The dramatic change in mass-loss rate supports the hypothesis of eruptive/explosive mass loss immediately preceding the SN. Again, owing to the striking similarities shared with SN 1994W, both qualitatively and quantitatively, one arrives at a similar conclusion for the outer-wind parameters of SN 2011ht.

The very steep plateau edges in the light curves of SNe 2011ht, 1994W, and 2009kn are rather unusual for SNe II<sub>n</sub>, which normally exhibit a slow, steady decline. In

the case of SN 1994W, Chugai et al. (2004) interpreted this characteristic as the result of the SN shock wave reaching the edge of a dense CSM envelope, while Dessart et al. (2009) favored simple photospheric contraction as a result of hydrogen cooling to recombination temperature. The latter scenario was also favored by Kankare et al. (2012) in the case of SN 2009kn. However, both of these scenarios may play a role in producing the sharp plateau edge. As the SN shock propagates through the dense CSM, the cool dense shell (CDS) that develops at the SN-CSM interface will create an optically thick barrier that masks the inner high-velocity ejecta. Once the presumed “edge” of the dense CSM envelope is reached, the CDS should rapidly expand and become optically thin. By this time, if the inner ejecta have already cooled below the recombination temperature of hydrogen ( $\sim 6000 \text{ K}$ ), the explosion should become transparent to the observer rather instantly, resulting in a rapid drop in continuum flux, and an instantaneous transition into the nebular phase. Since the radiative energy of the inner ejecta is dominated by the thermalization of radioactively generated photons, a sufficiently low mass of radioactive  $^{56}\text{Ni}$  could potentially result in such a scenario by allowing the interior to rapidly cool and become transparent before the CDS reaches the edge of the CSM and thins out. Low  $^{56}\text{Ni}$  mass is also consistent with the small velocity widths of the emission lines observed during the nebular phases of SNe 2011ht, 1994W, and 2009kn (Maguire et al. 2012). We demonstrate below that the late-time luminosity of SN 2011ht does indeed imply an exceptionally low mass of radioactive  $^{56}\text{Ni}$  synthesized in the explosion.

## 4.2 Low $^{56}\text{Ni}$ Mass

The subluminal decay tails of SNe 2011ht, 1994W, and 2009kn imply a relatively low yield of  $^{56}\text{Ni}$ . Since radioactivity provides the thermal energy of the ejecta, a larger synthesized mass of  $^{56}\text{Ni}$  will not only result in a brighter decay tail in the late-time light curve, but also extend the hydrogen recombination time scale, resulting in a shallower plateau edge and smoother transition into the nebular phase, as exhibited by the light curve of SN 1987A included in Figure 3. SNe that yield a small  $^{56}\text{Ni}$  mass exhibit the most subluminal decay tails and the sharpest plateau edges (e.g., see Elmhamdi et al. 2003). Thus, SNe 2011ht, 1994W, and 2009kn appear fully consistent with low  $^{56}\text{Ni}$ -yield core-collapse explosions in every respect.

According to Sutherland & Wheeler (1984), the relationship between the bolometric luminosity of the decay tail and the total mass of  $^{56}\text{Ni}$  can be expressed as

$$L = 1.42 \times 10^{43} \text{ erg s}^{-1} e^{-t/111 \text{ days}} M_{\text{Ni}}/M_\odot, \quad (2)$$

assuming 100%  $\gamma$ -ray deposition efficiency into the SN envelope. For the moment, let us assume that the light-curve tail of SN 2011ht is dominated by  $^{56}\text{Co}$  decay, ignoring potential contribution from residual CSM interaction at late times. The bolometric values we derived via SED integration imply a total luminosity of  $L_{\text{bol}} = 3.3 \times 10^{40} \text{ erg s}^{-1}$  for SN 2011ht on day 166, which implies a  $^{56}\text{Ni}$  mass of  $\sim 0.01 \text{ M}_\odot$  using Equation 2. This is a significantly lower  $^{56}\text{Ni}$  mass than for most normal SNe II-P, which typically exhibit values in the range  $0.06\text{--}0.10 \text{ M}_\odot$  (Turatto et al. 1990; Sollerman 2002).

One can also estimate the  $^{56}\text{Ni}$  mass by direct comparison of decay-tail luminosity to that of the nearby SN 1987A, which provides a reliable benchmark, owing to its well-constrained distance and luminosity. The mass of  $^{56}\text{Ni}$  produced by SN 1987A is  $0.071^{+0.019}_{-0.016} M_{\odot}$  (Suntzeff & Bouchet 1990). The luminosity of SN 1987A on day 203 was  $1.6 \times 10^{41} \text{ erg s}^{-1}$  (Suntzeff et al. 1991). By direct comparison, the luminosity ratio of 0.035 implies an initial  $^{56}\text{Ni}$  mass of  $0.01 \pm 0.005 M_{\odot}$  for SN 2011ht, which is fully consistent with the value from the method of Sutherland & Wheeler (1984). The SN 1987A comparison method was used by Kankare et al. (2012) to estimate a value of  $0.03 M_{\odot}$  for SN 2009kn, which was regarded as a lower limit, since the shallower decline rate for this SN indicates the likelihood that persistent CSM interaction continued well into the nebular phase and thus contributed to the late-time bolometric luminosity.

Note that for the above analysis we assumed that the explosion date is the discovery date. We expect that the uncertainty in explosion date is likely to be less than 1–2 weeks, since the early UV rise was observed by Roming et al. (2012). A two-week difference would alter the derived  $^{56}\text{Ni}$  mass by only 14%, which does not change our conclusion of low  $^{56}\text{Ni}$  yield.

Note that had we not considered the total optical-IR SED luminosity of SN 2011ht, and instead only used the optical photometry, we would have significantly underestimated the bolometric luminosity and, hence, the  $^{56}\text{Ni}$  mass. For example, using its absolute magnitude of  $M_V = -10.67$  mag on day 203 and adopting a bolometric correction of  $-0.45$  mag for the nebular phase (Bersten & Hamuy 2009), the total luminosity calculated for day 203 would be  $5.7 \times 10^{39} \text{ erg s}^{-1}$ , implying a factor of 4–5 lower  $^{56}\text{Ni}$  mass of  $2.4 \times 10^{-3} M_{\odot}$ . The underestimated value matches the *lower* end of the range derived for SN 1994W by Sollerman et al. (1998), who did not have IR measurements at their disposal. Thus, the true  $^{56}\text{Ni}$  mass of SN 1994W was probably closer to the *upper* end of their derived range ( $0.015 M_{\odot}$ ), which accounted for dust formation. They considered dust as a potential cause for the unusually steep late-time decline of the optical light curve.

### 4.3 The Possible Influence of Dust

For SN 1994W, dust formation could have been more tightly constrained if multi-band optical and IR coverage had been obtained at late times. For SN 2011ht, we were fortunate to have obtained multi-band optical measurements during the nebular phase, which can be combined with the late-time *JHKLM* measurements of SN 2011ht reported by Humphreys et al. (2012). The IR data, included in Figure 2, unambiguously demonstrate that substantial flux has shifted into the IR after the plateau phase, and this has been attributed to the formation of dust. However, if the steep optical decline were caused by extinction from such dust, then we might have expected substantial reddening to be observed in the  $V - R$  and  $V - I$  colors between days 141 and 203. As shown in Figure 2, no such reddening is observed after the plateau phase ends. In fact, the colors appear to flatten out and become slightly bluer, probably because the continuum during the end of the plateau, which exhibited strong line

blanketing at the blue end of the spectrum, has dropped out almost completely by day 147.

The photometric data are perhaps a bit too sparse at late times to justify making any definitive conclusions about dust formation and increasing extinction. However, the late-time luminosity ratio of  $H\alpha$  and  $H\beta$  emission, shown in Figure 8, does appear to be consistent with increasing reddening, as the last  $H\beta$  measurement after day 200 deviates from  $H\alpha$  more extremely than for earlier epochs. Alternatively, in the optically thin regime, collisional excitation can result in significant deviations from Case B recombination, which will also result in a decreasing  $H\beta$  luminosity; this could be important for the nebular phase. We note that if extinction by dust is important for  $H\alpha$ , then the estimated CSM wind-density parameters that are based on the luminosity of this line could be significantly underestimated for SN 2011ht and SN 1994W.

In conclusion, although the cause of the steep optical decline of SN 2011ht remains unclear, the hypothesis of dust formation is consistent with the data. The steep optical decline during the nebular phase would thus likely to be the result of the absorption and thermal reprocessing of photons. Such dust could have condensed following the steep drop in luminosity after the plateau, although the rapid time scale over which grains would have had to grow is difficult to reconcile (Humphreys et al. 2012). Whatever the case, the properties of SNe 2011ht, 1994W, and 2009kn underscore the importance of obtaining IR photometry to accompany optical measurements during both the plateau phase and later nebular phases, so that the full bolometric luminosity can be precisely estimated and the possible influence of dust can be realized.

### 4.4 The Nature of the Explosion and the Progenitor

The results of our observations and analysis imply a  $^{56}\text{Ni}$  mass of  $\sim 0.01 M_{\odot}$  for SN 2011ht. This low amount has important implications for the nature of the progenitor. The lowest  $^{56}\text{Ni}$  yields may result from the lowest-mass stars believed to be capable of undergoing core collapse. Stars with initial masses of 8–10  $M_{\odot}$  cannot produce an Fe core. Instead, they are thought to end their lives as super-asymptotic-giant-branch (SAGB) stars which develop electron-degenerate O-Ne-Mg cores (Barkat 1974; Nomoto 1984). The favored core-collapse mechanism in this case is electron capture on  $^{24}\text{Mg}$  and  $^{20}\text{Ne}$ , which triggers collapse before the onset of explosive O burning (Miyaji et al. 1980). Owing to the low overall mass and the neutron richness of the ejecta, nucleosynthesis models for electron-capture SNe predict low  $^{56}\text{Ni}$  yields, perhaps as small as  $0.002 M_{\odot}$  (Wanaajo et al. 2009), but certainly  $< 0.015 M_{\odot}$  (Kitaura et al. 2006).

The low-luminosity SN II-P 2005cs had a progenitor mass of  $9^{+3}_{-2} M_{\odot}$ , based on pre-SN images of the nearby host galaxy Messier 51 (Maund et al. 2005), and a very low  $^{56}\text{Ni}$  mass of  $3 \times 10^{-3} M_{\odot}$  (Pastorello et al. 2009). The light curve of this SN, included in Figure 3, exhibits a steep plateau edge and a subluminal decline, similar to SN 2011ht and SN 1994W. Based on the low progenitor mass and the meager  $^{56}\text{Ni}$  yield, SN 2005cs was considered a viable candidate for an electron-capture SN. However, the IR colors of the

progenitor appear inconsistent with those of an SAGB star (Eldridge et al. 2007).

If the low  $^{56}\text{Ni}$  yields of SNe 2011ht, 1994W, and 2009kn are the outcome of electron-capture SNe with 8–10  $M_{\odot}$  SAGB progenitors, then the CSM ejected in the several years before core collapse could have resulted from explosive instabilities that occur during the final nuclear burning stages (e.g., Woosley & Weaver 1979). Models of the final stages of SAGB stars also predict enhanced pre-SN mass-loss rates of  $\sim 10^{-4} M_{\odot} \text{ yr}^{-1}$  (e.g., Poelarends et al. 2008, and references therein), capable of producing dense CSM. However, the 500–800  $\text{km s}^{-1}$  velocity of the P-Cygni absorption components of SNe 2011ht, 1994W, and 2009kn are significantly faster than the observed wind velocities of SAGB stars ( $\sim 10 \text{ km s}^{-1}$ ). Still, there is no particular reason to suspect that eruptive pre-SN mass loss from SAGB stars, perhaps the result of final nuclear flashes, should share the low outflow velocities of earlier, steady SAGB winds.

Alternatively, low  $^{56}\text{Ni}$  yield can result if a substantial fraction of the inner core ejecta does not achieve the escape velocity necessary for a successful explosion and thus falls back onto the compact remnant, perhaps descending into a black hole. If this is the case, then the progenitors of SN 2011ht and SN 1994W could have been substantially more massive than 8–10  $M_{\odot}$ , perhaps having initial masses of 30  $M_{\odot}$  or more (Fryer 1999). Consider the case of the jet-powered SN 2010jp, which has been suggested to possibly mark the formation of a black hole (Smith et al. 2012b). This SN II<sub>n</sub> exhibited a steeply declining decay tail with a low overall luminosity, which constrained the  $^{56}\text{Ni}$  mass to  $< 0.003 M_{\odot}$ . Black hole formation is likely preceded by substantial fallback of SN ejecta, so low  $^{56}\text{Ni}$  masses are to be expected in such a scenario.

There is the possibility that SN 2011ht represents a non-terminal scenario. Dessart et al. (2009) suggested that SN 1994W could have resulted from the interaction of colliding circumstellar shells that were ejected from consecutive explosive mass-loss events, where the more recent ejection has a higher velocity and catches up with the slower outer shell, creating a luminous collision by conversion of kinetic energy into UV-optical-IR light. If SN 2011ht was the result of an LBV eruption, however, it would be a rather remarkable set of coincidences for the end of the plateau phase to occur at  $\sim 120$  days, which is a very typical time scale for SNe II-P, and for the late-time bolometric decline to be consistent with the  $^{56}\text{Co}$  decay rate. The uncanny spectroscopic and photometric similarity of SN 2011ht and SN 1994W to SN 2009kn, which was almost certainly a bona fide core-collapse event, would also be a rather remarkable coincidence.

Arguments in favor of the nonterminal LBV scenario (e.g., Humphreys et al. 2012) are based on a plausibility argument, and thus provide insufficient evidence against core collapse. The lack of observational signatures from high-velocity material in the spectra of SNe 2011ht, 1994W, and 2009kn can be explained by the presence of an optically thick CDS that remains present during the entire plateau phase, which masked emission from inner high-velocity material. A similar process was invoked to explain the spectrum of the luminous SN 2006gy, shown in Figure 10, which shares many spectral similarities with SN 2011ht, SN 1994W, and SN 2009kn. For these SNe, by the time the CDS thinned out,

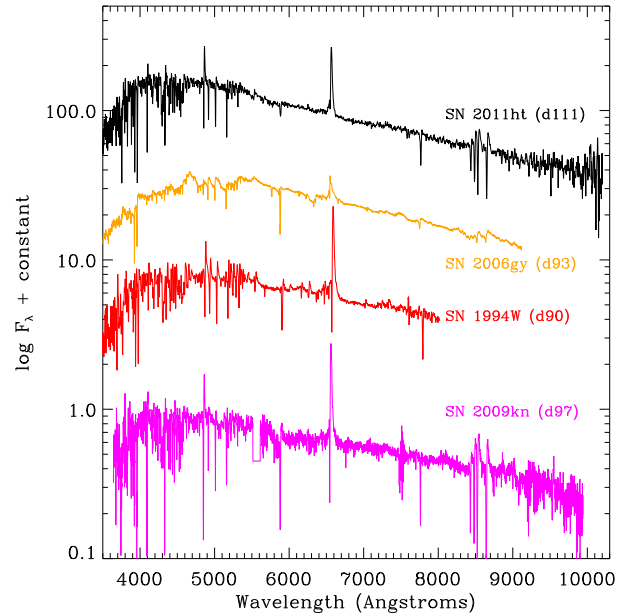


**Figure 10.** Spectra of SN 2011ht on day 111 compared with the very luminous SN 2006gy on day 93, in addition to SN 1994W on day 90 and SN 2009kn on day 97. Although SN 2006gy exhibited a much stronger continuum component, which diluted the emission lines, its overall spectrum signifies cool dense gas, similar to the other three SNe.

the explosion could have cooled and become transparent, never revealing the observational signature of high-velocity ejecta. As we pointed out earlier, the exceptionally low  $^{56}\text{Ni}$  masses derived for SN 2011ht, SN 1994W, and, to a lesser extent, SN 2009kn, could allow for such rapid cooling and optical thinning of the ejecta, as the radioactive energy source was weak in these cases compared with normal SNe II. Finally, the interpretation of the SN 2011ht spectrum as the result of a radiatively driven “opaque wind” is not physically plausible. Assuming that Thompson scattering dominates the optical depth ( $\kappa_e = 0.34$ ), the SN 2011ht peak luminosity of  $L_{\text{peak}} = (5 \pm 2) \times 10^{42} \text{ erg s}^{-1}$  would imply an Eddington factor of  $\Gamma = (\kappa_e L) / 4\pi G M c \approx 1000$ , which would undoubtedly result in explosive mass loss, not a wind, as suggested by Humphreys et al. (2012).

The only reliable means to observationally discriminate between the possibility of electron-capture SNe, a fallback scenario, or surviving LBVs would be the detection of the progenitor from deep pre-SN space-based images of the host galaxy, or an upper limit in the case of the electron-capture scenario. Unfortunately, pre-existing SDSS images of the SN 2011ht host, UGC 4560, do not place firm constraints on the nature of the progenitor, other than the fact that it could not be a progenitor as luminous as  $\eta$  Car (Romig et al. 2012). However, LBVs on the fainter end of the distribution may be possible. Still, scenarios that produce multiple massive shell ejections, such as the pulsational pair instability (Woosley et al. 2007), require extremely massive stars ( $> 90 M_{\odot}$ ), which would also be extremely luminous. This scenario would also seem unlikely to produce three SNe having such similar observational characteristics.

## 5 CONCLUSIONS

We have presented extensive photometric and spectroscopic coverage of SN 2011ht. Our data complement those published by Roming et al. (2012) and Humphreys et al. (2012), but we arrive at somewhat different conclusions. This SN IIn shares with SN 1994W and SN 2009kn an unusual combination of properties, including a well-defined and abruptly ending plateau phase dominated by CSM interaction, and an exceptionally low yield of  $^{56}\text{Ni}$ . The results of our analysis, particularly the late-time bolometric decline being consistent with the  $^{56}\text{Co}$  decay rate, supports the hypothesis that SN 2011ht, like SN 2009kn, was a core-collapse SN, and not the result of a super-Eddington wind. The more exotic scenario of multiple colliding LBV shells (Dessart et al. 2009) is a little more difficult to firmly rule out, although there is no reason why such a scenario should produce the plateau duration of  $\sim 120$  days, which is so common among SNe II-P, or a late-time decline that is consistent with  $^{56}\text{Co}$  decay.

The most likely scenario is that SN 2011ht was a bona fide core-collapse SN that produced a low  $^{56}\text{Ni}$  yield and exploded into dense CSM. Its discovery marks the third addition to an unusual group of SNe IIn, including SN 1994W and SN 2009kn. We argue that this justifies the designation of a new subclass of SNe exhibiting Type IIn spectra and plateau light curves, which we propose be Type IIn-P.

The low synthesized mass of  $^{56}\text{Ni}$  for these events highlights the possibility that they are either the result of electron-capture SNe from 8–10  $M_{\odot}$  progenitors, or explosions which experienced substantial fallback of their inner metal-rich ejecta. The only way to effectively discriminate between these possibilities for similar SNe in the future will be the detection of their stellar progenitors in pre-existing space-based images of their host galaxies. Additional members of the Type IIn-P class will undoubtedly emerge from future all-sky surveys, such as Pan-STARRS, LSST, and SkyMapper, and will enable the physical nature of these explosions to be elucidated more completely. Statistics for their rates and host-galaxy environments may also help discriminate between the two likely origins.

## ACKNOWLEDGMENTS

This work is based in part on observations made at the the MMT Observatory, a joint facility of the Smithsonian Institution and the University of Arizona, and at the Lick Observatory, which is owned and operated by the University of California. Some of the data presented herein were obtained at the W. M. Keck Observatory, which is operated as a scientific partnership among the California Institute of Technology, the University of California, and NASA; the observatory was made possible by the generous financial support of the W. M. Keck Foundation. Infrared data herein were obtained using PAIRITEL, which is operated by the Smithsonian Astrophysical Observatory (SAO) and was made possible by a grant from the Harvard University Milton Fund, the camera loan from the University of Virginia, and the continued support of the SAO and UC Berkeley. We thank the staffs at these observatories for their efficient assistance. We are grateful to P. E. Nugent, D. Cohen, B. Y. Choi, M. Ellison, M. Mason, A. Wilkins, P. Blanchard, M. T. Kandrashoff,

and O. Nayak for their help with observations at Keck and Lick. We thank P. Milne for conducting photometric observations of SN 2011ht at two epochs. We also thank J. Bloom, A. A. Miller, D. Starr, and C. Blake for facilitating PAIRITEL data contributions. We also thank E. Kankare for providing several epochs of spectra of SN 2009kn for our comparison. The supernova research of A.V.F.’s group at U.C. Berkeley is supported by Gary & Cynthia Bengier, the Richard & Rhoda Goldman Fund, the Christopher R. Redlich Fund, the TABASGO Foundation, and NSF grants AST-0908886 and AST-1211916.

## REFERENCES

- Barkat, Z. 1971, *ApJ*, 163, 433
- Begelman, M. C., & Sarazin, C. L. 1986, *ApJ*, 302, L59
- Bersten, M. C., & Hamuy, M. 2009, *ApJ*, 701, 200
- Bloom, J. S., Starr, D. L., Blake, C. H., Skrutskie, M. F., & Falco, E. E. 2006, in *Astronomical Data Analysis Software and Systems XV*, ed. C. Gabriel, et al. (SF: ASP, vol. 351), 751
- Bowen, D. V., Roth, K. C., Meyer, D. M., & Blades, J. C. 2000, *ApJ*, 536, 225
- Chugai, N. N. 1990, *Sov. Astron. Let.*, 16, 457
- Chugai, N. N. 2001, *MNRAS*, 326, 1448
- Chugai, N. N. 2009, *MNRAS*, 400, 866
- Chugai, N. N., Blinnikov, S. I., Cumming, R. J., et al. 2004, *MNRAS*, 352, 1213
- Cooke, J. 2008, *ApJ*, 677, 137
- Dessart, L., Hillier, D. J., Gezari, S., Basa, S., & Matheson, T. 2009, *MNRAS*, 394, 21
- Di Carlo, E., Massi, F., Valentini, G., et al. 2002, *ApJ*, 573, 144
- Eldridge, J. J., Mattila, S., & Smartt, S. J. 2007, *MNRAS*, 376, L52
- Elmhamdi, A., Tsvetkov, D., Danziger, I. J., & Kordi, A. 2011, *ApJ*, 731, 129
- Filippenko, A. V. 1982, *PASP*, 94, 715
- Filippenko, A. V. 1997, *ARAA*, 35, 309
- Filippenko, A. V., & Sargent, W. L. W. 1985, *Nature*, 316, 407
- Foley, R. J., Smith, N., Ganeshalingam, M., et al. 2007, *APJL*, 657, L105
- Foley, R. J., Chornock, R., Filippenko, A. V., et al. 2009, *AJ*, 138, 376
- Fryer, C. L. 1999, *ApJ*, 522, 413
- Gal-Yam, A., & Leonard, D. C. 2009, *Nature*, 458, 865
- Gao, Y., & Solomon, P. M. 2004, *ApJS*, 152, 63
- Hamuy, M., Suntzeff, N. B., Bravo, J., & Phillips, M. M. 1990, *PASP*, 102, 888
- Humphreys, R. M., Davidson, K., Jones, T. J., et al. 2012, *arXiv:1207.5755*
- Humphreys, R. M., & Davidson, K. 1994, *PASP*, 106, 1025
- Kitaura, F. S., Janka, H.-T., & Hillebrandt, W. 2006, *A&A*, 450, 345
- Leonard, D. C., Filippenko, A. V., Barth, A. J., & Matheson, T. 2000, *ApJ*, 536, 239
- Leonard, D. C., Filippenko, A. V., Gates, E. L., et al. 2002, *PASP*, 114, 35
- Li, W., Leaman, J., Chornock, R., et al. 2011, *MNRAS*, 412, 1441

- Maguire, K., Jerkstrand, A., Smartt, S. J., et al. 2012, MNRAS, 420, 3451
- Mauerhan, J., & Smith, N. 2012, arXiv:1204.1610
- MacFadyen, A. I., & Woosley, S. E. 1999, ApJ, 524, 262
- Miller J. S., & Stone, R. P. S. 1993, Lick Obs. Tech. Rep. 66 (Santa Cruz: Lick Obs.)
- Miyaji, S., Nomoto, K., Yokoi, K., & Sugimoto, D. 1980, PASJ, 32, 303
- Nomoto, K. 1984, ApJ, 277, 791
- Oke, J. B., Cohen, J. G., Carr, M., et al. 1995, PASP, 107, 375
- Pastorello, A., Sauer, D., Taubenberger, S., et al. 2006, MNRAS, 370, 1752
- Pastorello, A., Stanishev, V., Smartt, S. J., & Fraser, M. 2011, CBET, 2851
- Pastorello, A., Valenti, S., Zampieri, L., et al. 2009, MNRAS, 394, 2266
- Pastorello, A., Zampieri, L., Turatto, M., et al. 2004, MNRAS, 347, 74
- Pooley, D. et al. 2012, ATEL, 4062
- Roming, P., 2011, ATEL, 3690
- Roming, P. W. A., Pritchard, T. A., Prieto, J. L., et al. 2012, arXiv:1202.4840
- Silverman, J. M., Foley, R. J., Filippenko, A. V., et al. 2012, arXiv:1202.2128
- Smith, N., Cenko, S. B., Butler, N., et al. 2012b, MNRAS, 420, 1135
- Smith, N., Chornock, R., Li, W., et al. 2008, ApJ, 686, 467
- Smith, N., Li, W., Filippenko, A. V., & Chornock, R. 2011, MNRAS, 412, 1522
- Smith, N., Li, W., Foley, R. J., et al. 2007, ApJ, 666, 1116
- Smith, N., Mauerhan, J. C., Silverman, J. M., et al. 2012a, arXiv:1204.0043
- Smith, N., & Owocki, S. P. 2006, ApJ, 645, L45
- Smith, N., Silverman, J. M., Chornock, R., et al. 2009, ApJ, 695, 1334
- Sollerman, J. 2002, NewAR, 46, 493
- Sollerman, J., Cumming, R. J., & Lundqvist, P. 1998, ApJ, 493, 933
- Suntzeff, N. B., & Bouchet, P. 1990, AJ, 99, 650
- Suntzeff, N. B., Phillips, M. M., Depoy, D. L., Elias, J. H., & Walker, A. R. 1991, AJ, 102, 1118
- Sutherland, P. G., & Wheeler, J. C. 1984, ApJ, 280, 282
- Turatto, M., Cappellaro, E., Danziger, I. J., et al. 1993, MNRAS, 262, 128
- Turatto, M., Mazzali, P. A., Young, T. R., et al. 1998, ApJL, 498, L129
- Utrobin, V. P., & Chugai, N. N. 2008, A&A, 491, 507
- Utrobin, V. P., Chugai, N. N., & Pastorello, A. 2007, A&A, 475, 973
- Van Dyk, S. D., Peng, C. Y., King, J. Y., et al. 2000, PASP, 112, 1532
- Wanajo, S., Nomoto, K., Janka, H.-T., Kitaura, F. S., Müller, B. 2009, ApJ, 695, 208
- Weiler, K. W., van Dyk, S. D., Discenna, J. L., Panagia, N., & Sramek, R. A. 1991, ApJ, 380, 161
- Woosley, S. E., Blinnikov, S., & Heger, A. 2007, Nature, 450, 390
- Woosley, S. E., & Weaver, T. A. 1980, ApJ, 238, 1017
- Yaron, O., & Gal-Yam, A. 2012, arXiv:1204.1891
- Zwicky, F. 1964, ApJ, 139, 514